RSC Advances

PAPER

View Article Online
View Journal | View Issue

Cite this: *RSC Adv.*, 2021, **11**, 10468

Copolymer chain formation of 2-oxazolines by *in situ* ^{1}H-NMR spectroscopy: dependence of sequential composition on substituent structure and monomer ratios†

Sabina Abbrent, *[a] Andrii Mahun,[ab] Miroslava Dušková Smrčková,[a] Libor Kobera,[a] Rafał Konefał,[a] Peter Černoch,[a] Karel Dušek[a] and Jiří Brus[a]

Received 24th February 2021
Accepted 3rd March 2021

DOI: 10.1039/d1ra01509e

rsc.li/rsc-advances

In situ ^{1}H NMR characterization of copolymerization reactions of various 2-oxazoline monomers at different molar ratios offers detailed insight into the build-up and composition of the polymer chains. Various 2-oxazolines were copolymerized in one single solvent, butyronitrile, with 2-dec-9′-enyl-2-oxazoline, where the double bond allows for post-polymerization modification and can function as a crosslinking unit to form polymer networks. The types of the monomers and their molar ratios in the feed have a strong effect on the microstructure of the forming copolymer chains. Copolymers comprising 2-dec-9′-enyl-2-oxazoline and either 2-ethyl-, 2-isopropyl-, 2-butyl-, 2-heptyl, 2-nonyl- or 2-phenyl-2-oxazoline, show significant differences in sequential structure of copolymers ranging from block to gradient and random ordering of the monomer units. ^{1}H NMR was found to be a powerful tool to uncover detailed oxazoline copolymerization kinetics and evolution of chain composition.

Introduction

Poly(2-oxazoline)s (POx) have attracted the attention of scientists particularly as a class of polymer materials with highly tunable physicochemical properties.[1,2] They have shown great potential for biomedical applications[3–9] because their aqueous solutions or hydrogels exhibit the volume phase transition of lower critical solution temperature (LCST) type. However, these materials can also be utilized as catalysts,[10,11] photolithographic matrices for electronics,[1] protective coatings,[12] and electronic insulators.[13] Versatility of oxazoline polymers,[14,15] their chemical and physical properties, "green" production[16,17] and biocompatibility also suggest their possible use in renewable power source applications. The requirements for materials used for polymer electrolytes are strict and plentiful including electrochemical stability, good ionic conduction coupled with electronic insulation, wide electrochemical window, robustness against electrical, mechanical, and thermal stresses and last but not least environmental friendliness and biological and chemical stability.[18]

The use of POx-based polymers for any application demands detailed exploration of reaction kinetics, copolymerization behavior and influence of (co)polymer structure on its physicochemical behavior and related processes.[19–27] Generally, the copolymerization of various types of 2-oxazoline (Ox) monomers is feasible due to their structural similarity. Oxazoline copolymers ranging from random through gradient to block architectures can be prepared depending on the copolymerization behavior leading to different self-organization in solution.[28,29]

Polyoxazolines can be easily synthesized by living cationic ring-opening polymerization (CROP) of 2-substituted-2-oxazolines, usually initiated by tosylates or other electrophilic compounds.[8,19,30,31] Well-defined POx with relatively narrow dispersity index ($Đ$) ~1.2 or even less[27] are obtained. Variation of the Ox-substituent controls hydrophilicity[32,33] of the final polymer or allows for post-polymerization modification of the POx backbone.[34,35]

Although many kinetic studies of POx can be found in literature, the results are often incomparable, as different conditions are frequently used; above all various solvents, initiators and polymerization temperatures[36–38] (comprehensive literature overview can be found in ESI Table S1†). In recent years many studies have been conducted using the microwave technique,[39] which shows significant differences from the reflux method.[40] Furthermore, available kinetic studies of (co)polymerization of Ox monomers are usually based on running series of individual reactions or sampling from the reaction mixture with subsequent analysis by combination of gas chromatography (GC), size exclusion chromatography (SEC) and nuclear magnetic resonance (NMR).[22,24,41,42]

In this contribution, we have used *in situ* ^{1}H NMR measurements which enabled frequent, quick and detailed

[a]*Institute of Macromolecular Chemistry of the Czech Academy of Sciences, Heyrovskeho nam. 2, 162 06 Prague 6, Czech Republic*

[b]*Department of Physical and Macromolecular Chemistry, Faculty of Science, Charles University, Hlavova 8, 128 40 Prague 2, Czech Republic*

† Electronic supplementary information (ESI) available. See DOI: 10.1039/d1ra01509e

tracking (herein with 10 minutes interval) of sample composition throughout the whole polymerization process from its initiation to full conversion of the monomers in a closed, undisturbed system.[43–46]

Here, we have focused on copolymerization of series of 2-substituted-2-oxazolines (2-ethyl-, 2-isopropyl-, 2-butyl-, 2-heptyl-, 2-nonyl-, and 2-phenyl-) with 2-dec-9′-enyl-2-oxazoline (DecOx), see Fig. 1. DecOx was chosen for its C=C double bond to be later used for crosslinking of the copolymer to form network polymer films. Special attention was paid to selection of solvent suitable for this study (see the Experimental section) which would sufficiently well dissolve both monomers and copolymers and at the same time not impede polymerization kinetics. This contribution presents a novel approach using *in situ* ^{1}H NMR spectroscopy for the above specified POx monomers to study the influence of their molar ratio in feed on sequential composition of the forming copolymer chain.

Experimental

Materials

2-Ethyl-2-oxazoline, 2-phenyl-2-oxazoline, butyronitrile, acetonitrile, ethyl acetate, dimethyl carbonate, methyl *p*-toluene sulfonate, ethanolamine, titanium(IV) oxide, barium oxide, benzoyl chloride, decanoic acid, 10-undecenoic acid and octanoic acid were purchased from Merck and cadmium acetate from Acros Organics. 2-Heptyl-2-oxazoline, 2-nonyl-2-oxazoline, 2-dec-9′-enyl-2-oxazoline were prepared according to literature.[16,47] 2-isopropyl-2-oxazoline and 2-butyl-2-oxazoline were synthesized following literature.[48,49] Butyronitrile was stored over molecular sieve 3 Å. Each 2-oxazoline monomer was vacuum-distilled twice: first over barium oxide, then after addition of 1 vol% of benzoyl chloride. Freshly distilled monomers were stored over argon at 4 °C. All other chemicals were used as received.

Choice of solvent

A series of various solvents was considered and tested. Acetonitrile, ethyl acetate, and dimethyl carbonate, widely used for POx studies, were rejected due to poor solubility of the more hydrophobic POx species and their precipitation during polymerization. Common chlorinated solvents were found excellent for all studied POx; however, methylene chloride was rejected due its low boiling point; tetrachloroethylene, because of its broad interfering signal in ^{1}H NMR spectra as well as for significantly higher dispersity of prepared POx polymers ($Đ \approx 1.4$) compared to other solvents ($Đ = 1.1$–1.3). Sulfolane[25] was rejected because of its melting point over ambient temperature and related handling difficulties. Finally, butyronitrile[24,40] was chosen as it dissolves all used POx species, has reasonable boiling point and suitable chemical shift and relative intensity of its peaks in ^{1}H NMR spectra. Also, contrary to chlorinated solvents, it can be considered a "green material".

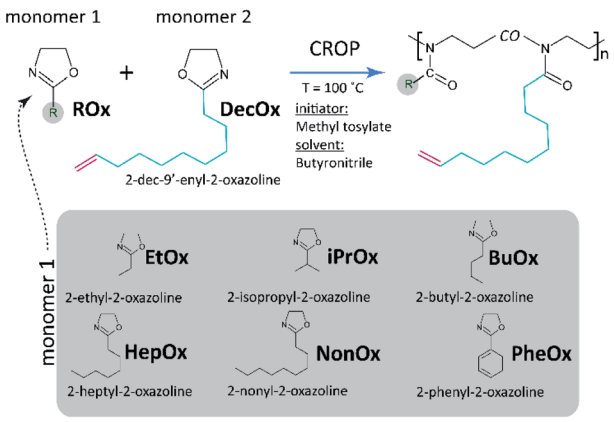

Fig. 1 Simplified reaction scheme indicating cationic ring-opening (co)polymerization (CROP) of 2-oxazolines and list of comonomers copolymerized with 2-dec-9′-enyl-2-oxazoline used in this study.

Polymerizations

All glassware (vials, NMR-tubes, stoppers, syringes, needles, magnetic stirrers *etc.*) were dried in oven at 120 °C overnight and directly before experiments let to cool in vacuum desiccator and transferred into glove box with argon atmosphere. Homo- and copolymers were synthesized by living CROP (see Fig. 1).[19] Briefly, solvent, monomers and initiator were added into a dry vial with a magnetic stirrer in glovebox under argon atmosphere and crimped. The mixture was well-homogenized and still in glovebox, 0.8 mL aliquots were transferred into dry 5 mm NMR tube *via* clean and dry glass syringe with needle and sealed with a tight stopper. Immediately after removal from glovebox, filled NMR tubes were flame-sealed and stored in freezer until measurement. The rest of polymerization mixture in the tube was conventionally polymerized in microwave reactor at 100 °C within 4 hours and terminated with adding of 3-fold excess of piperidine. Methyl *p*-toluene sulfonate was used as initiator at a ratio of monomer(s)-to-initiator 100 : 1 in all cases. NMR-observed polymerizations were conducted directly in NMR chamber preheated to 100 °C ± 0.5 °C.

Monomer(s) concentration in solvent was adjusted to 3 M for 2-ethyl-, 2-isopropyl- and 2-*n*-butyl-2-oxazoline-based mixtures and to 2 M for 2-heptyl-, 2-nonyl-, 2-phenyl- and 2-dec-9′-enyl-2-oxazoline in order to provide comparable (weight) amounts of the monomers in the corresponding reaction solutions.[22] Three different monomer mixtures with ratios of the selected 2-oxazoline and DecOx were prepared and coded 90 : 10, 80 : 20 and 60 : 40. These code numbers mean the targeted ranges of molar ratios which naturally differ somewhat from the exact value from sample to sample and are given in Table 1. These ratios were chosen based on the consideration of future cross-linking using DecOx double bond and thus optimization of polymer network structure (not part of this publication). The polymerization temperature of 100 °C was chosen as a compromise ensuring both a relatively high reaction rate and a low extent of side-reactions.[50] After the polymerization, samples were analyzed by SEC.

Instrumental measurements

SEC analysis was performed on a setup equipped with PLgel 5 μm 100 Å and DeltaGel Mixed-B columns, RI detector and

Table 1 Polymer characteristics experimentally determined by ^{1}H NMR and SEC: molecular weight averages and dispersity index $Đ$[a]

Intended molar ratio ROx : DecOx		Real molar ratio ROx : DecOx						
Substituent R		Ethyl-	Isopropyl-	Butyl-	Heptyl-	Nonyl-	Phenyl-	Decenyl-
Molar ratio	**100 : 0**							
NMR	$\bar{X}_{n(i)}/\bar{X}_{n(f)}$	65/62	78/75	65/65	67/68	60/56	55/40	70/70
	$\bar{M}_{id}/\bar{M}_n$ (10^3)	6.4/6.1	8.8/8.5	8.3/8.3	11.5/11.5	11.8/11.0	8.1/5.9	14.6/14.6
SEC	$\bar{M}_w/\bar{M}_n$ (10^3)	10.2/9.8	13.1/10.9	11.5/10.0	15.0/12.6	17.8/15.4	9.5/8.7	14.9/13.0
	$Đ$	1.05	1.11	1.13	1.14	1.16	1.09	1.14
Molar ratio	**90 : 10**	**86 : 14**	**84 : 16**	**85 : 15**	**89 : 11**	**79 : 21**	**91 : 9**	—
NMR	$\bar{X}_{n(i)}/\bar{X}_{n(f)}$	70/60	60/60	60/58	67/68	62/55	78/35	—
	$\bar{M}_{id}/\bar{M}_n$ (10^3)	6.9/5.9	6.8/6.8	7.6/7.4	11.5/11.5	12.2/10.8	11.4/5.1	—
SEC	$\bar{M}_w/\bar{M}_n$ (10^3)	10.5/9.9	9.5/8.5	12.3/10.9	14.6/12.8	19.9/18.3	18.9/17.2	—
	$Đ$	1.06	1.11	1.11	1.15	1.09	1.11	—
Molar ratio	**80 : 20**	**77 : 23**	**75 : 25**	**74 : 26**	**76 : 24**	**67 : 33**	**81 : 19**	—
NMR	$\bar{X}_{n(i)}/\bar{X}_{n(f)}$	66/59	67/69	65/63	79/73	82/72	50/35	—
	$\bar{M}_{id}/\bar{M}_n$ (10^3)	6.5/5.8	7.9/7.9	8.2/8.0	13.2/12.3	16.2/14.2	7.4/5.1	—
SEC	$\bar{M}_w/\bar{M}_n$ (10^3)	12.0/11.4	13.2/11.8	12.5/10.0	16.6/13.4	18.8/17.4	15.7/14.2	—
	$Đ$	1.05	1.10	1.15	1.18	1.08	1.10	—
Molar ratio	**60 : 40**	**58 : 42**	**60 : 40**	**57 : 43**	**54 : 46**	**52 : 48**	**68 : 32**	
NMR	$\bar{X}_{n(i)}/\bar{X}_{n(f)}$	68/63	70/70	55/55	79/65	70/70	65/40	—
	$\bar{M}_{id}/\bar{M}_n$ (10^3)	6.7/6.2	7.9/7.9	7.0/7.0	13.3/11.0	13.8/13.8	9.6/5.9	—
SEC	$\bar{M}_w/\bar{M}_n$ (10^3)	14.3/13.5	13.2/12.3	14.0/12.4	16.8/14.8	18.8/17.4	17.5/15.4	—
	$Đ$	1.05	1.09	1.11	1.14	1.08	1.13	—

[a] Intended and real molar ratios of monomers, the average number of repeating monomer units per chain – average degree of polymerization $\bar{X}_{n(i)}$ as calculated from NMR spectra from monomer to initiator ratio (index i – initial) and polymer to initiator ratio (index f – final) (as compared to intended monomer/initiator ratio 100/1). The average ideal molecular weight of polymer chain (M_{id}) as obtained from $\bar{X}_{n(i)}$ and $\bar{M}_n$ obtained from $\bar{X}_{n(f)}$ and real molar ratios obtained from ratios of integrated peak areas (experimental error of NMR estimations 5%). $\bar{M}_n$ and $\bar{M}_w$ values and $Đ$ are obtained from SEC. For definitions see ESI Table S2.

mixture of chloroform–triethylamine–isopropanol 94 : 4 : 2 as the mobile phase with flow rate of 1 mL min^{-1}. The system was calibrated with poly(methyl methacrylate) standards.

^{1}H NMR spectra were acquired with Bruker Avance III 600 spectrometer operating at Larmor frequency of $\nu(^1\mathrm{H}) = 600.2$ MHz. The width of 90° pulse was 10 μs, recycle delay (D_1) 10 s. Each sample was placed in spectrometer preheated to 100 °C. Deuterated *N*,*N*-dimethylformamide-d$_7$ (DMF) and hexamethyldisiloxane (HMDS) in a capillary were placed inside the NMR tube before its filling and sealing and used as external reference. Measurements were conducted every 10 minutes (data are averages over two scans) until full conversion of monomers was reached (usually 3–16 h) using a "*zgdelay*" pulse program (see ESI Section 2† for details).

Microwave polymerizations were carried out in automated microwave reactor in closed vials with magnetic stirrer (Robot Sixty, Biotage, Sweden) at 100 °C and reaction time of 4–10 hours.

Results and discussion

NMR measurements evaluations

Initially, monomer conversions were measured using ^{1}H NMR spectroscopy and obtained from the integral ratios of resonances corresponding to each monomer and its polymer backbone (–CH_2CH_2–).[51] ^{1}H NMR spectra for all monomers are shown in Fig. 2 and individual shifts for each monomer given in ESI (Section 3†) were assigned according to literature.[36,52] During polymerization, slight shifts of the individual peaks were observed, caused by changes in solubility and chemical environment of the samples.

Individual peaks obtained and identified for the copolymers are shown in Fig. 3a. DecOx double bonds found at 5.6 and 4.8 ppm are clearly distinguished and remain unchanged during the polymerization reaction. They can be used for calibration of the three changing oxazoline ring peaks.

At the same time, the peaks corresponding to the oxazoline rings (marked as closed oxazoline ring in Fig. 3) represent the

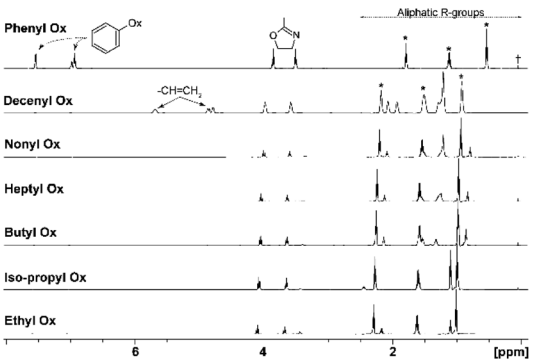

Fig. 2 ^{1}H NMR spectra of monomers, exact chemical shifts are given in ESI,† peaks with asterisk corresponding to solvent butyronitrile, the cross corresponds to standard HMDS set at 0.05 ppm. Chemical shift of signals corresponding to butyronitrile in ^{1}H NMR spectrum of PheOx to lower frequency is caused by strong shielding effects of the aromatic rings.

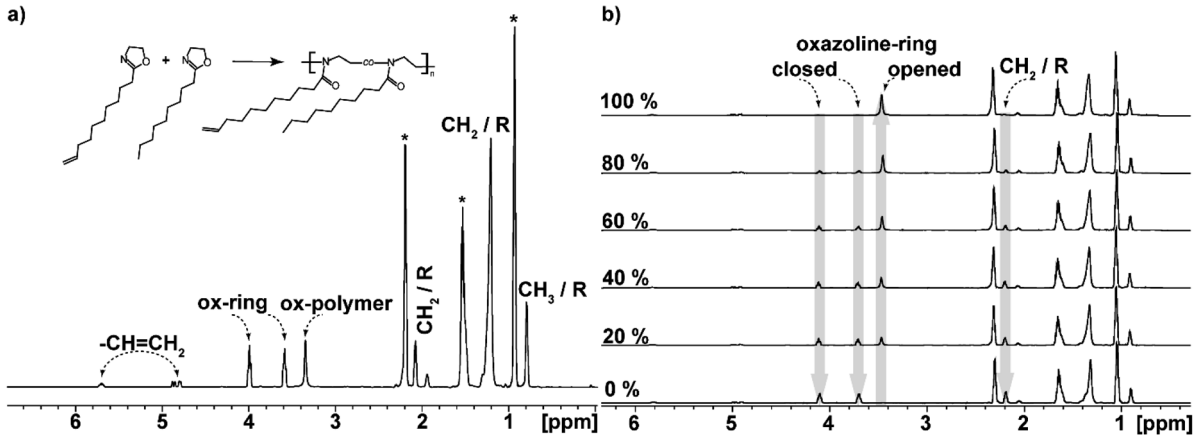

Fig. 3 (a) Comonomer peak assignment for the NonOx/DecOx 90 : 10 mixture, R representing the side group substituents, the asterisks denote the solvent. (b) Monomer conversion in percentage as seen in time, arrows highlight the changing peaks used for evaluation, "closed" represents the oxazoline ring of the monomers, "opened" represents one unit of the formed polymer.

monomers while the POx units are designated as opened oxazoline rings or polymer. Intensities of these peaks change during polymerization reaction; the two monomer peaks decrease while the polymer peak grows as shown in Fig. 3b.

The polymerization degree was calculated from ratio of integral intensity of the butyronitrile solvent peak, which remained constant throughout the reaction, to changing monomer and polymer signals. Using the constant solvent peak as an internal standard, also the real initial ratios of monomers in their mixtures were established from the ratio of DecOx to ROx integrated peaks at $t = 0$ (from spectra of initial mixture). The experimental molar ratio of monomers to initiator was also determined from the initial spectra and used for estimate of ideal copolymer chain degree of polymerization defined as $\bar{X}_{n(i)}$ given for individual mixtures in Table 1. By comparing the initiator peaks (at ~6.9 and 7.5 ppm corresponding to the two peaks of benzene ring of reacted initiator) to polymer peaks at full monomer conversion, estimation of real average chain length and molecular weight of the copolymers can be made, see values of $\bar{X}_{n(f)}$, $\bar{M}_{id}$, $\bar{M}_n$ in Table 1. The difference between $\bar{X}_{n(i)}$ and $\bar{X}_{n(f)}$ values roughly corresponds to the degree of side reactions in the particular comonomer mixture.

Molecular weights and dispersities obtained by SEC of the polymerized content of NMR-tubes and microwave vials for the NonOx/DecOx system are shown in ESI Section 5† for comparison and show only minor differences. The polymerization time was set to four hours, which according to NMR-based results corresponded to full conversion for all reaction mixtures, except for PheOx systems that demanded ten hours reaction times. The series of experiments conducted in NMR tubes clearly afford better control of the polymerization process, including suppression of side reactions often occurring during microwave polymerization,[19,53] especially at high conversions and temperature fluctuations observed in microwave at larger volumes of reaction mixtures. Similar characteristics (monomodal, narrow distribution) were observed for all reactions conducted in NMR tubes. At the chosen temperature of 100 °C, side reactions are insignificant. Furthermore, *in situ* NMR-based study of POx kinetics proceeds in a closed system without any interruptions and external influences can be dismissed. On the other hand, the limitation of this method is the decreased accuracy of reading peak intensities at extreme points of the reaction course (very small peaks from the polymer initially and the vanishing peaks of the monomer at the end of the polymerization). Therefore, to ensure reproducibility, at least two measurements were conducted and the deconvolutions were determined from mean values of three independent calculations; the differences corresponded to 5% error (for data see ESI Section 6†).

In the case of the comonomers, with exception of PheOx/DecOx (see the shift in Fig. 2), the monomer peaks in NMR spectra overlap. In order to obtain concentration data for each monomer and each measurement, deconvolution analysis was used and the individual peaks and their intensities could thus be obtained as seen in Fig. 4. The fitting of appropriate ^{1}H NMR signal(s) was carried out in TOP SPIN DNMR module by the following steps: firstly, the exact values of ^{1}H NMR shift and J-coupling of each monomer separately were defined in

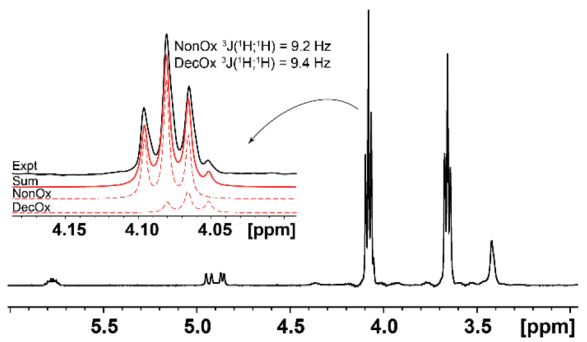

Fig. 4 Relevant section of ^{1}H NMR spectrum of a copolymer (here NonOx/DecOx 90 : 10 after 20 minutes of reaction). Decreasing monomer signals are seen at 4.1 and 3.7, while the growing peak at 3.4 ppm relates to polymerized species. Signals from the two monomers overlap but could be separated by deconvolution (see inset with each of the monomers in dashed lines, the sum of deconvolution in solid red and original spectral line in black).

"multiplet analysis – mana" plugin included in TOP SPIN software. Secondly, these parameters were transferred to DNMR module for a two-component system. In view of the fact that the analyzed signal(s) correspond to $-CH_2-$ groups, the pseudo-spin was defined as 1 (this agrees with DNMR Lineshape Analysis Software Manual). Then, the intensities of individual peaks were estimated based on expected copolymer ratio and final shape was calculated using automatic procedure of the DNMR module. Fitting of two curves in DNMR employs the minimization of the least-square difference function.[54] The final copolymer ratio was obtained as calculated integral areas.

For the analysis of measured spectra following denotations and definitions were used (for overview see ESI Table S2†) c corresponds to relative monomer concentration proportional to molar concentration of both monomers and is obtained directly from ^{1}H NMR spectra (by comparison of integrals of signals from monomers to internal standard); P is defined as the molar concentrations of both polymerized units, obtained directly from NMR spectra from integral ratios of signals from polymer to internal standard. It applies that $c + P$ is constant throughout the reaction.

Monomer molar fractions in the reacting monomer mixture at time t with respect to the initial amount of both monomers, defined as

$$x_{1+2} = \frac{c}{(c)_0} \tag{1}$$

were calculated, where $(c)_0$ is the initial monomer concentration (0 minutes of reaction) and c corresponds to monomer content at time t (obtained for every ten minutes of reaction time).

The fraction of both polymerized monomer units p_{1+2} is defined as

$$p_{1+2} = \frac{P}{P_{\alpha=1}} \tag{2}$$

where $P_{\alpha=1}$ is the corresponding integral of polymer peak at full conversion. Molar conversion of oxazoline groups of both monomers, α, is expressed as

$$\alpha = 1 - \frac{c}{(c)_0} \tag{3}$$

By deconvolution of the peaks corresponding to c, molar fractions (f_1, f_2) of each monomer with respect to monomer mixture were obtained, where

$$f_1 = \frac{c_1}{c}; f_2 = \frac{c_2}{c} \text{ and } f_1 + f_2 = 1 \tag{4}$$

Molar fractions of each monomer in the whole mixture x_1 and x_2, defined as

$$x_1 = x_{1+2} \times f_1,\ x_2 = x_{1+2} \times f_2 \tag{5}$$

where it applies that $x_1 + x_2 + p_{1+2} = 1$.

Conversions of monomers 1 and 2, α_1, α_2 are calculated as

$$\alpha_1 = \frac{c_1}{(c_1)_0},\ \alpha_2 = \frac{c_2}{(c_2)_0} \tag{6}$$

Molar fractions of monomer units in polymer cannot be obtained directly from the spectra as the polymer species are represented by one single broad peak. However, these values are calculated from consumption of monomers as the integral fractions F_1 and F_2

$$F_1 = \frac{(c_1)_0 - c_1}{((c_1)_0 - c_1) + ((c_2)_0 - c_2)} \tag{7}$$

with $F_1 + F_2 = 1$. The composition of instantaneously formed polymer (within the 10 minutes interval) is defined by

$$\Delta F_1 = \frac{(c_1)_{t+\Delta t} - (c_1)_t}{((c_1)_{t+\Delta t} - (c_1)_t) + ((c_2)_{t+\Delta t} - (c_2)_t)} \tag{8}$$

where again $\Delta F_1 + \Delta F_2 = 1$.

Homopolymerization and copolymerization

The homopolymerization rate, as obtained from integration of the increasing ^{1}H NMR spectral peak corresponding to the open-ring species, is characterized by reaction half-times (Table 2). Different polymerization rates as dependent on monomer substituents are clearly documented. The monomer conversion as a function of time during homopolymerization is also shown in ESI Fig. S3.† The half-time values are around 40 minutes for oxazolines with aliphatic substituents, increasing slightly with the length of the chain. Isopropyl-, decenyl- and phenyl-oxazolines show longer half-times. Monomers containing phenyl- and isopropyl-groups react slower than the aliphatic side-chain species; isopropyl has an electron-donating effect while phenyl weakens polarization (basicity of N) by a mesomeric effect. Alkyls provide weaker electron donating effect, somewhat decreasing with alkyl length, but there is also a steric effect that depends not only on the alkyl length and structure but also on the environment. Also, one should consider effect of dilution by material in alkyl chains.

When copolymerization of the oxazolines with DecOx is considered, the half-times are dependent on both monomer substituent type and ratio, also shown in Fig. 5. In the investigated group of six oxazoline comonomers, the short aliphatic side chains (EtOx and BuOx) in copolymerization with DecOx show almost identical half-times as their corresponding

Table 2 Half-times of reactions $t_{1/2}$ (min) for homopolymers (first column) and for copolymers with 2-dec-9′-enyl-2-oxazoline. Experimental error ~5%

	$t_{1/2}$ [min]			
	Molar ratio ROx : DecOx			
ROx	100 : 0	90 : 10	80 : 20	60 : 40
EtOx	34	32	33	33
IPrOx	65	54	38	43
BuOx	35	32	32	33
HepOx	43	38	53	53
NonOx	37	58	57	55
PheOx	79	190	210	175
DecOx	78	—	—	—

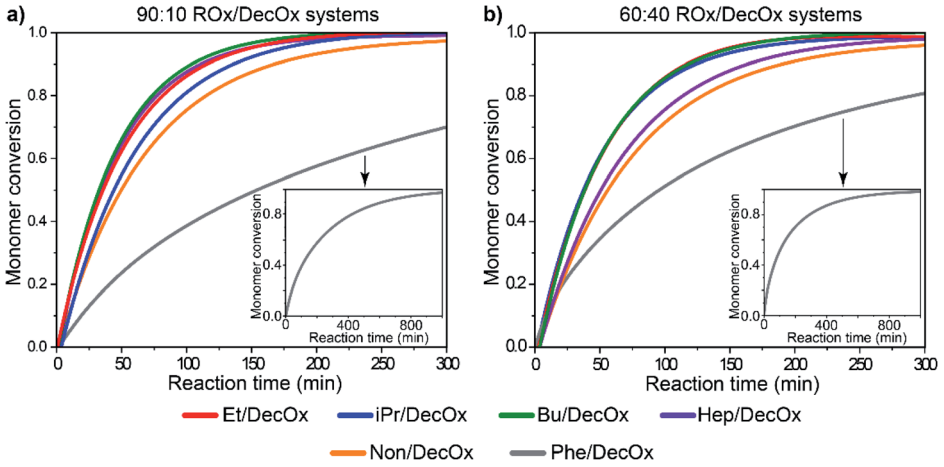

Fig. 5 Monomer conversion as a function of time for (a) 90 : 10 and (b) 60 : 40 monomer ratios of oxazoline mixtures, showing full conversion of the systems and full conversion of 2-phenyl-2-oxazoline in the insets. Detailed graphs with data point are depicted in ESI Fig S4.†

homopolymers. Longer aliphatic species in side chain increase the polymerization times with their increasing concentration in feed (HepOx, NonOx). The combination of PheOx with DecOx in the feed is quite distinct: for the three studied ratios, the half-times are more than doubled compared to homopolymers of both monomers. On the other hand, presence of isopropyl substituent causes shortening of the observed copolymerization rate. Clearly, the half-times of copolymerizing systems result from complex mechanism and mutual influences of both comonomers. However, the single half-time value provides only first approximation on reaction rate but little information on the individual monomer consumption and monomer sequencing in the copolymer chain.

At this point, it would be interesting to view the rates of consumption of each monomer in the copolymerizing systems. Therefore, we performed deconvolution of the individual monomer peaks in the ^{1}H NMR spectra (as described in detail above) which enabled direct observation of monomer consumption from the feed. This data provides basis for detailed analysis of the copolymerization kinetics. Firstly, Table 1 presents average chain lengths and molecular weights of the homopolymers and copolymers ($\bar{M}_n$) obtained experimentally from ^{1}H NMR, calculated from integral peak ratios of the polymer at full conversion and monomer composition according to eqn (1) and (2) and the same parameters obtained from SEC with materials prepared in microwave for comparison.

Full monomer conversion α (eqn (3)) for mixtures has been confirmed by the disappearance of ^{1}H NMR peaks corresponding to the oxazoline rings (Fig. 3b).

Changes of copolymer composition in the course of copolymerization

The reactivity ratios (copolymerization parameters) usually serve for better understanding of the copolymerization reactions and allow determination of composition of the copolymer structure. However, for our systems, the copolymerization parameters could not be obtained. Indeed, Fineman–Ross model was used for the calculations, however, no satisfactory results were obtained, see ESI Section 9.† One factor is the limited number of monomer ratios but also the resulting fits of obtained copolymerization parameters show no linear dependency for most copolymers. Instead, the above defined parameters f_1, F_1 and ΔF_1 were used directly for detailed description of the copolymerization reactions in the whole conversion range.

As a first step, experimental data in Table 2 were extended to include half-times of each monomer in the pair. Interesting observations can be made by comparing these individual half-times: for example, if the monomer half-time in a mixture significantly differs from its homopolymerization, it is a sign of the effect of environment and dilution by the other comonomer on its reactivity in CROP, such as DecOx in EtOx/DecOx (90 : 10) or PheOx in PheOx/DecOx (all ratios), *cf.* see ESI Table S5.† The interpretation of individual half-times for various monomer ratios is, however, not straightforward. The ^{1}H NMR analysis enables much more detailed insight into the copolymer chain composition evolving in time. As a first step, monomer relative molar concentrations x_1 and x_2 were obtained from the deconvolution of monomer peaks and calculated according to eqn (1) and (5). (For plots with experimental data see ESI, Fig. S5 and S6†). Then, the composition of the copolymer was characterized as it developed in time by the composition of monomer mixture in feed characterized by monomer molar fractions f_1,f_2, integral content of polymerized units in copolymer chains from beginning of copolymerization (F_1, F_2), differential copolymer composition added during a time interval (ΔF_1, ΔF_2) and conversions of monomers 1 and 2 (α_1, α_2) (eqn (4)–(8)). It is especially F_1, F_2 and α_1, α_2 as they change in time that offer information about the sequential structure (random, gradient, block) of the copolymers. Below, we will discuss the sequential structure development for each comonomer pair separately, illustrated by panel with four diagrams showing dependence of monomer 1 expressed by f_1, F_1 and ΔF_1 (Fig. 6–11(a), (b) and (c) respectively) – while the parameters for DecOx (monomer 2) are superfluous being complement to 1 (see variable definition above or in ESI Table S2†). In Fig. 6–11(d) the conversion of each

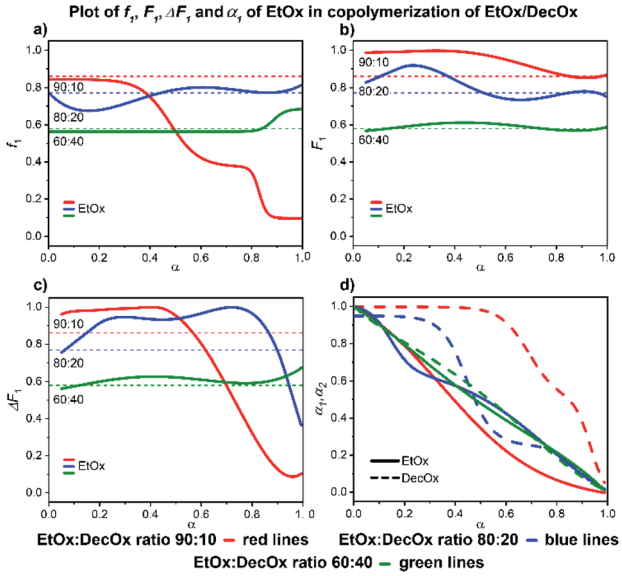

Fig. 6 2-Ethyl-2-oxazoline/2-decenyl-2-oxazoline system. Dependence of EtOx (monomer 1) expressed as (a) f_1, (b) F_1, (c) ΔF_1 and (d) α_1, α_2 plotted as functions of monomer conversion α and fitted by 4th polynomial function for easy viewing. The horizontal lines in (a–c) denote the starting monomer mixture composition determined experimentally from ^{1}H NMR spectra, in (d) full lines represent EtOx and dashed lines DecOx monomers. Graphs including experimental points are presented in ESI.†

monomer in time α_1, α_2 included for each system shows mutual rate of the incorporation of monomers into the polymer chain providing direct information on the type of forming copolymer. The individual conversions α_1, α_2 are plotted on the scale 0–1 for each monomer in order to compare the relative rates of their consumption. Changes of monomer molar fractions x_1 andx_2 obtained from deconvolution of ^{1}H NMR spectra plotted as a function of time and conversion α that were used for calculations of described parameters are given in ESI, Fig. S5 and S6.† Also, graphs shown below but including data points for clarity can be found in ESI, Fig. S7–S10.†

2-Ethyl-2-oxazoline/2-decenyl-2-oxazoline. The behavior is clearly different for each ratio of the two monomers (Fig. 6). The DecOx-rich 60 : 40 monomer mixture gives rise to almost perfectly random copolymer with identical molar ratios of monomer units in the monomer mixture and in the copolymer as well until 90% conversion after which a short DecOx-rich block is formed (*cf.* Fig. 6d). The ethyl richer mixtures behave differently: the 80 : 20 mixture initially forms an EtOx-rich polymer which transforms to random copolymer structure after ~35% conversion is reached. The EtOx-rich 90 : 10 mixture shows a steep gradient copolymer formation with EtOx-rich block up to 50% conversion transforming gradually into DecOx-richer gradient copolymer with almost complete depletion of ethyl before 90% conversion is reached (Fig. 6c).

Slower reaction of DecOx compared to ethyl in the mixtures 90 : 10 and 80 : 20 can be the reason for the initial tendency to form EtOx-rich block. The formation of DecOx-rich copolymer is the consequence of depletion of monomer mixture by ethyl at higher conversions.

2-iPropyl-2-oxazoline/2-decenyl-2-oxazoline. In case of iPrOx/DecOx mixtures the behavior is different compared to the Et/DecOx one (Fig. 7). The polymerization of iPrOx is considerably slower than that of EtOx (Table 2) but still somewhat faster than that of DecOx. Disregarding the first 20% conversion (affected by distribution of initiating sites among the comonomers) and the region beyond 80%, the copolymerization is almost ideally random.

2-Butyl-2-oxazoline/2-decenyl-2-oxazoline. The BuOx/DecOx systems show a strong tendency towards formation of BuOx blocks which increases with decreasing amount of DecOx in the system (Fig. 8). As a consequence of depletion of BuOx monomers, DecOx blocks are formed at the later stages. Comparing these three copolymers of DecOx with oxazolines having small alkyl groups, the isopropyl group is the strongest electron donor, followed by ethyl and butyl groups and the homopolymerization rates correspond to that order (iPrOx is the slowest).

2-Heptyl-2-oxazoline/2-decenyl-2-oxazoline. In case of the HepOx/DecOx samples (Fig. 9), a faster initial reaction of DecOx is observed, the rate increases with ratio HepOx : DecOx and result in formation of gradient copolymer almost of diblock-type at the 60 : 40 ratio. The copolymer formed at the ratio 80 : 20 is almost random and a composition with weak gradient is observed at the ratio 90 : 10.

2-Nonyl-2-oxazoline/2-decenyl-2-oxazoline. In the case of NonOx/DecOx copolymers (Fig. 10), basically the same reaction rates were observed for all three ratios (disregarding the low conversion part, Fig. 10b) leading to gradual enrichment of

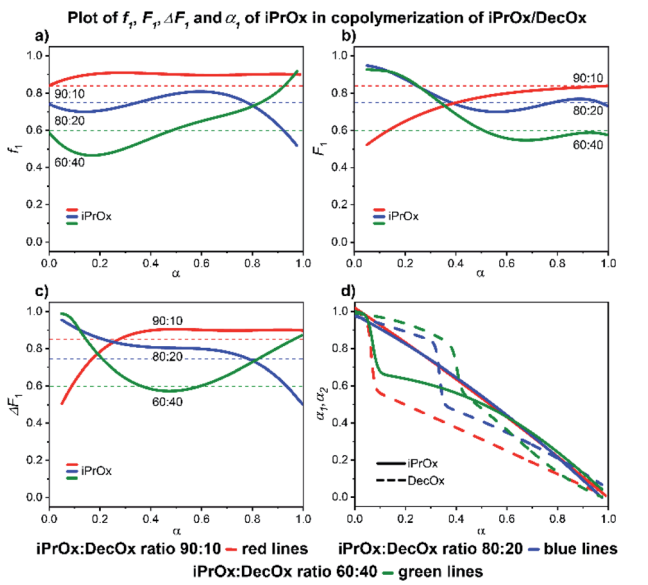

Fig. 7 2-iPropyl-2-oxazoline/2-decenyl-2-oxazoline system. Dependence of iPrOx (monomer 1) expressed as (a) f_1, (b) F_1, (c) ΔF_1 and (d) α_1, α_2 plotted as functions of monomer conversion α and fitted by 4th polynomial function for easy viewing. The horizontal lines in (a–c) denote the starting monomer mixture composition determined experimentally from ^{1}H NMR spectra, in (d) full lines represent iPrOx and dashed lines DecOx monomers. Graphs including experimental points are presented in ESI.†

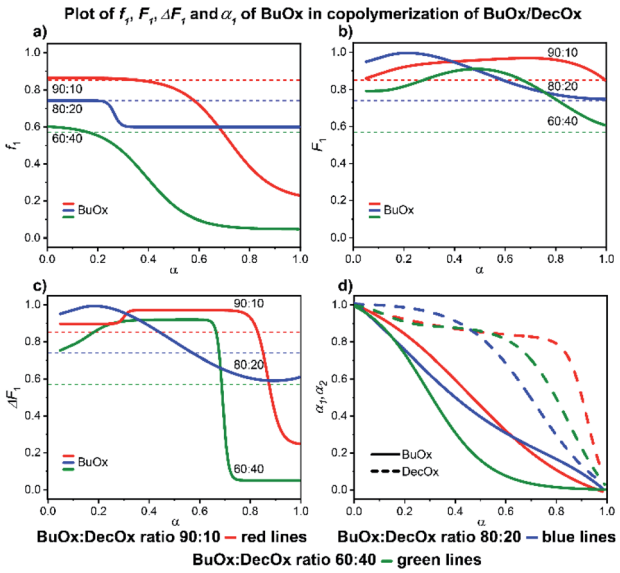

Fig. 8 2-Butyl-2-oxazoline/2-decenyl-2-oxazoline system. Dependence of BuOx (monomer 1) expressed as (a) f_1, (b) F_1, (c) ΔF_1 and (d) α_1, α_2 plotted as functions of monomer conversion α and fitted by 4th polynomial function for easy viewing. The horizontal lines in (a–c) denote the starting monomer mixture composition determined experimentally from ^{1}H NMR spectra, in (d) full lines represent BuOx and dashed lines DecOx monomers. Graphs including experimental points are presented in ESI.†

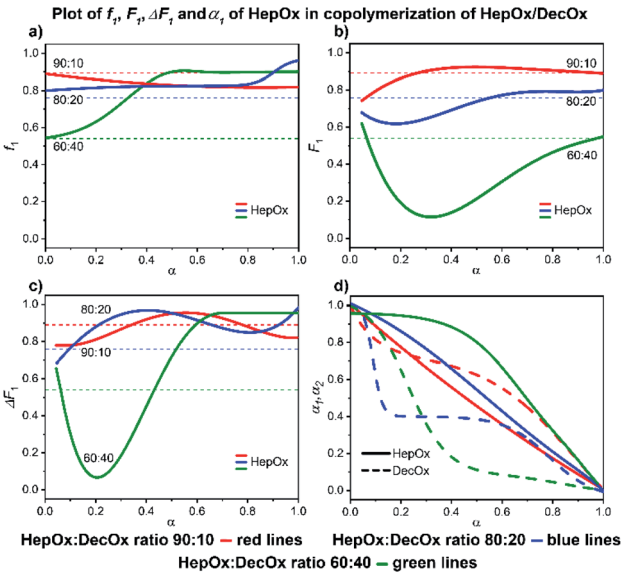

Fig. 9 2-Heptyl-2-oxazoline/2-decenyl-2-oxazoline system. Dependence of HepOx (monomer 1) expressed as (a) f_1, (b) F_1, (c) ΔF_1 and (d) α_1, α_2 plotted as functions of monomer conversion α and fitted by 4th polynomial function for easy viewing. The horizontal lines in (a–c) denote the starting monomer mixture composition determined experimentally from ^{1}H NMR spectra, in (d) full lines represent HepOx and dashed lines DecOx monomers. Graphs including experimental points are presented in ESI.†

monomer feed by the slower reacting DecOx. For the 60 : 40 system, a complete consumption of NonOx is observed at 80% conversion, followed by formation of a short DecOx-block sequence. The 80 : 20 sample shows a sudden, unexpected, increase of NonOx monomer at 80% conversion possibly related to formation of a heterogeneous phase (Fig. 10a).

2-Phenyl-2-oxazoline/2-decenyl-2-oxazoline. Typical for the block-copolymer formation is the Phe/DecOx system as was already described in the literature.[29,36] The initial faster reaction of DecOx results in complete depletion of the monomer at 40 (90 : 10 and 80 : 20 mixtures) and 60% conversion (60 : 40 mixture), respectively; thereafter the poly(PheOx) block is formed (Fig. 11). The initial polymer composition corresponds to short poly(DecOx) block followed by a gradient copolymer and finally longer poly(PheOx) block.

Factors controlling compositional changes. The evolution of composition of the growing chains during RO copolymerization is controlled by rates the comonomers react with activated chain ends. The respective rate constants are a function of chemical reactivity of the component (induction or mesomeric effects) and by the effect of the local environment. In the present series, a different chemical reactivity is expected for the isopropyl side group (electron donating) and especially the phenyl substituent; the other substituents are long hydrocarbon chains and differences in Ox group reactivity are small. The local environment effect is expected to be different: the activated chain ends are dissolved in mixtures of monomer and solvent (butyronitrile) the ratio of which changes during copolymerization.

Moreover, the spatial distribution of growth centers and monomer molecules can be non-random. The deviation from randomness can be caused by association (clustering) of polar

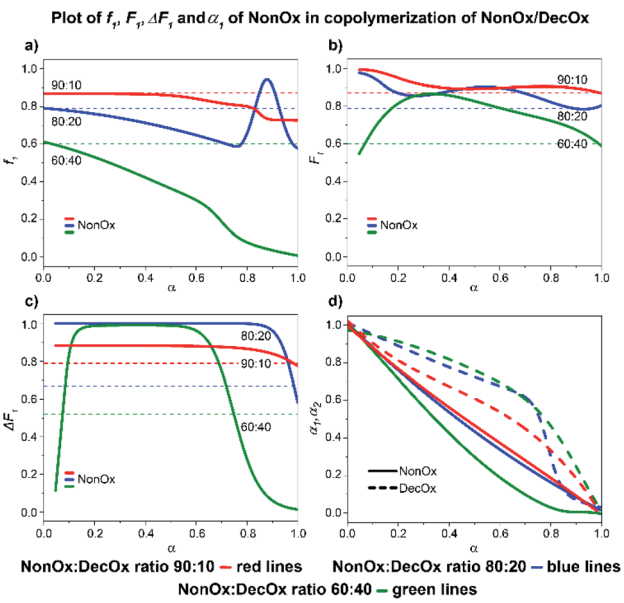

Fig. 10 2-Nonyl-2-oxazoline/2-decenyl-2-oxazoline system. Dependence of NonOx (monomer 1) expressed as(a) f_1, (b) F_1, (c) ΔF_1 and (d) α_1, α_2 plotted as functions of monomer conversion α and fitted by 4th polynomial function for easy viewing. The horizontal lines in (a–c) denote the starting monomer mixture composition determined experimentally from ^{1}H NMR spectra, in (d) full lines represent NonOx and dashed lines DecOx monomers. Graphs including experimental points are presented in ESI.†

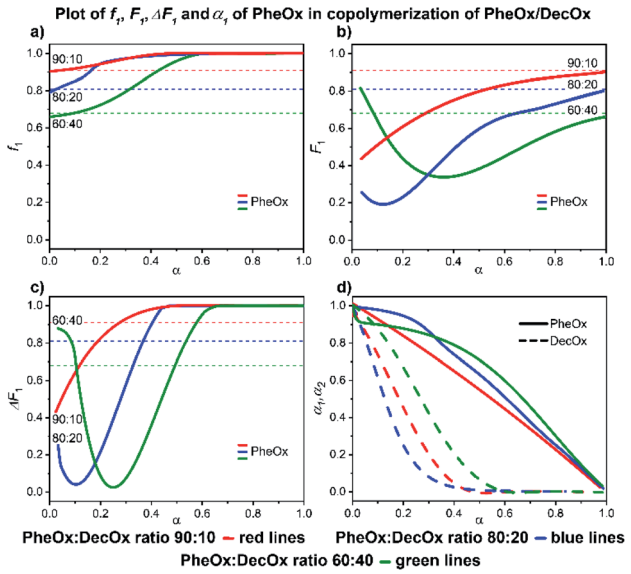

Fig. 11 2-Phenyl-2-oxazoline/2-decenyl-2-oxazoline system. Dependence of PheOx (monomer 1) expressed as (a) f_1, (b) F_1, (c) ΔF_1 and (d) α_1, α_2 plotted as functions of monomer conversion α and fitted by 4th polynomial function for easy viewing. The horizontal lines in (a–c) denote the starting monomer mixture composition determined experimentally from ^{1}H NMR spectra, in (d) full lines represent PheOx and dashed lines DecOx monomers. Graphs including experimental points are presented in ESI.†

and hydrophobic moieties. The tendency of aliphatic chain substituents to ordering by forming liquid-crystalline structures well documented in the literature can be another reason. Recently, the importance of the solvent effect on the sequential structure of Ox copolymers has been stressed.[55] At present, we have no experimental information about the level of aggregation and ordering in these systems.

A short analysis reveals the following features of DecOx-poor mixtures in butyronitrile: the tendencies to form block *versus* random copolymers are seen to vary for all monomer mixtures depending on the used ratios; a gradient copolymer is usually formed as a transition from block to random-copolymer structure. It can also be concluded that the more structurally similar comonomers form random rather than block-copolymer structures, as is the case for NonOx/DecOx and partly the HepOx/DecOx systems. On the other hand, the BuOx/DecOx and PheOx/DecOx show high tendency to form block copolymers, independently on their initial ratios.

The fact that the choice of substituent strongly influences the composition and microstructure of the forming copolymer has also been established for other Ox pairs.[48,56] However, it can be concluded that the monomer ratio has a strong effect on formation of the final polymer morphology. Furthermore, the degree of change in polymer microstructure depending on the initial monomer composition seems to depend on the length of the side-group compared to DecOx and hints to the effect of alignment of the paraffinic side chains. For instance, only 10% increase in the ratio of DecOx to EtOx in the initial mixture alters the polymer morphology from block to random copolymer. On the contrary, more electron-withdrawing substituents such as the phenyl-group clearly induce block copolymerization with small composition changes.

The experimental results obtained by *in situ* NMR method described here can be compared with predictions obtained by new "visualization method"[57,58] of monomer units sequential distribution based on the complete Mayo–Lewis scheme (not steady-state) amended by possible side reactions which uses Monte Carlo method for sampling growing chains. Alternatively, the NMR results could supplement the information by the environment effect not accounted for in the visualization method.

Conclusions

^{1}H NMR spectroscopy was found to be an efficient *in situ* tool for monitoring and characterization of substituted oxazoline copolymer chains. From the NMR spectra, exact *in situ* compositions of monomers mixture and the copolymer over the whole conversion range can be obtained in dependence on reaction time.

Our results confirm that in CROP the Ox monomers show unpredictable behavior in butyronitrile with a tendency toward formation of block, statistical or random copolymers. Final microstructure depends strongly on the nature of monomer side-group and molar ratio of the Ox comonomers. We also have observed that the usually used Fineman–Ross approximation can be used only in cases where the Ox co-monomers shows tendency to form the same copolymer type for all ratios (BuOx/DecOx and PheOx/DecOx systems in our work).

Future work in this direction should include characterization of aggregation and ordering phenomena to elucidate the changes in the microenvironment (SAXS, SANS, NMR) to complement the existing new computational method for predicting sequential distribution.[57] This will offer the tools to design specific polymer architecture including the cross-linkable copolymers. Such topological information coupled with exact statistical branching theory[59] will make possible in-depth description of the network structure.

Conflicts of interest

There are no conflicts to declare.

Acknowledgements

The authors acknowledge the Czech Science Foundation (grant no. GA18-12925S) for financial support. We also gratefully acknowledge the support of the Czech Academy of Sciences within the programme AV21 Strategy: RP10-Molecules and Materials for Life.

References

1 S. Kobayashi, *Polym. Sci. A Compr. Ref. 10 Vol. Set*, 2012, vol. 4, pp. 397–426.
2 R. Hoogenboom, *Macromol. Chem. Phys.*, 2007, **208**, 18–25.

3 O. Sedlacek, B. D. Monnery, S. K. Filippov, R. Hoogenboom and M. Hruby, *Macromol. Rapid Commun.*, 2012, **33**, 1648–1662.
4 T. X. Viegas, M. D. Bentley, J. M. Harris, Z. Fang, K. Yoon, B. Dizman, R. Weimer, A. Mero, G. Pasut and F. M. Veronese, *Bioconjugate Chem.*, 2011, **22**, 976–986.
5 R. Luxenhofer, Y. Han, A. Schulz, J. Tong, Z. He, A. V Kabanov and R. Jordan, *Macromol. Rapid Commun.*, 2012, **33**, 1613–1631.
6 R. Luxenhofer, *Novel Functional Poly (2-oxazoline) s as Potential Carriers for Biomedical Applications*, Technische Universitat Munchen, 2007.
7 M. Hruby, S. K. Filippov, J. Panek, M. Novakova, H. Mackova, J. Kucka, D. Vetvicka and K. Ulbrich, *Macromol. Biosci.*, 2010, **10**, 916–924.
8 L. Loukotová, J. Kučka, M. Rabyk, A. Höcherl, K. Venclíková, O. Janoušková, P. Páral, V. Kolářová, T. Heizer, L. Šefc, P. Štěpánek and M. Hrubý, *J. Controlled Release*, 2017, **268**, 78–91.
9 O. Policianova, J. Brus, M. Hruby and M. Urbanova, *Pharm. Dev. Technol.*, 2015, **20**, 935–940.
10 O. Sedláček, P. Černoch, J. Kučka, R. Konefal, P. Štěpánek, M. Vetrík, T. P. Lodge and M. Hrubý, *Langmuir*, 2016, **32**, 6115–6122.
11 A. Kozur, L. Burk, R. Thomann, P. J. Lutz and R. Mülhaupt, *Polymer*, 2019, **178**, 121553.
12 T. He, D. Jańczewski, S. Jana, A. Parthiban, S. Guo, X. Zhu, S. S.-C. C. Lee, F. J. Parra-Velandia, S. L.-M. M. Teo and G. J. Vancso, *J. Polym. Sci., Part A: Polym. Chem.*, 2016, **54**, 275–283.
13 M. Fimberger, I.-A. Tsekmes, R. Kochetov, J. Smit and F. Wiesbrock, *Polymers*, 2015, **8**, 6.
14 R. Hoogenboom, *Angew. Chem., Int. Ed.*, 2009, **48**, 7978–7994.
15 M. Glassner, M. Vergaelen and R. Hoogenboom, *Polym. Int.*, 2018, **67**, 32–45.
16 C. Petit, K. P. Luef, M. Edler, T. Griesser, J. M. Kremsner, A. Stadler, B. Grassl, S. S. Reynaud and F. Wiesbrock, *ChemSusChem*, 2015, **8**, 3401–3404.
17 H. Huang, R. Hoogenboom, M. A. M. Leenen, P. Guillet, A. M. Jonas, U. S. Schubert and J.-F. Gohy, *J. Am. Chem. Soc.*, 2006, **128**, 3784–3788.
18 K. Xu, *Chem. Rev.*, 2014, **114**, 11503–11618.
19 B. Verbraeken, B. D. Monnery, K. Lava and R. Hoogenboom, *Eur. Polym. J.*, 2017, **88**, 451–469.
20 F. Wiesbrock, R. Hoogenboom, M. Leenen, S. F. G. M. van Nispen, M. van der Loop, C. H. Abeln, A. M. J. van den Berg and U. S. Schubert, *Macromolecules*, 2005, **38**, 7957–7966.
21 M. Glassner, K. Lava, V. R. de la Rosa and R. Hoogenboom, *J. Polym. Sci., Part A: Polym. Chem.*, 2014, **52**, 3118–3122.
22 F. Wiesbrock, R. Hoogenboom, M. A. M. M. Leenen, M. A. R. R. Meier and U. S. Schubert, *Macromolecules*, 2005, **38**, 5025–5034.
23 S. Huber, N. Hutter and R. Jordan, *Colloid Polym. Sci.*, 2008, **286**, 1653–1661.
24 M. W. M. M. Fijten, J. M. Kranenburg, H. M. L. L. Thijs, R. M. Paulus, B. M. Van Lankvelt, J. De Hullu, M. Springintveld, D. J. G. G. Thielen, C. A. Tweedie, R. Hoogenboom, K. J. Van Vliet and U. S. Schubert, *Macromolecules*, 2007, **40**, 5879–5886.
25 O. Sedlacek, B. D. D. Monnery and R. Hoogenboom, *Polym. Chem.*, 2019, **10**, 1286–1290.
26 T. Lorson, M. M. Lübtow, E. Wegener, M. S. Haider, S. Borova, D. Nahm, R. Jordan, M. Sokolski-Papkov, A. V. Kabanov and R. Luxenhofer, *Biomaterials*, 2018, **178**, 204–280.
27 B. D. Monnery, V. V. Jerca, O. Sedlacek, B. Verbraeken, R. Cavill and R. Hoogenboom, *Angew. Chem., Int. Ed.*, 2018, **57**, 15400–15404.
28 K. Aoi and M. Okada, *Prog. Polym. Sci.*, 1996, **21**, 151–208.
29 R. Hoogenboom, M. W. M. Fijten, S. Wijnans, A. M. J. van den Berg, H. M. L. Thijs and U. S. Schubert, *J. Comb. Chem.*, 2006, **8**, 145–148.
30 S. Kobayashi, H. Uyama, Y. Narita and J. ichi Ishiyama, *Macromolecules*, 1992, **25**, 3232–3236.
31 R. Hoogenboom, H. M. L. M. L. Thijs, M. J. H. C. J. H. C. Jochems, B. M. M. van Lankvelt, M. W. M. W. M. Fijten and U. S. S. Schubert, *Chem. Commun.*, 2008, 5758.
32 R. Luxenhofer, A. Schulz, C. Roques, S. Li, T. K. Bronich, E. V. Batrakova, R. Jordan and A. V. Kabanov, *Biomaterials*, 2010, **31**, 4972–4979.
33 M. M. Bloksma, C. Weber, I. Y. Perevyazko, A. Kuse, A. Baumgärtel, A. Vollrath, R. Hoogenboom and U. S. Schubert, *Macromolecules*, 2011, **44**, 4057–4064.
34 O. Sedlacek, B. D. Monnery, J. Mattova, J. Kucka, J. Panek, O. Janouskova, A. Hocherl, B. Verbraeken, M. Vergaelen, M. Zadinova, R. Hoogenboom and M. Hruby, *Biomaterials*, 2017, **146**, 1–12.
35 O. Sedlacek, O. Janouskova, B. Verbraeken and R. Hoogenboom, *Biomacromolecules*, 2019, **20**, 222–230.
36 A. Dworak, B. Trzebicka, A. Kowalczuk, C. Tsvetanov and S. Rangelov, *Polimery*, 2014, **59**, 88–94.
37 S. Sinnwell and H. Ritter, *Macromol. Rapid Commun.*, 2005, **26**, 160–163.
38 K. Kempe, M. Lobert, R. Hoogenboom and U. S. Schubert, *J. Polym. Sci., Part A: Polym. Chem.*, 2009, **47**, 3829–3838.
39 A. Makino and S. Kobayashi, *J. Polym. Sci., Part A: Polym. Chem.*, 2010, **48**, 1251–1270.
40 F. Wiesbrock, R. Hoogenboom, C. H. Abeln and U. S. Schubert, *Macromol. Rapid Commun.*, 2004, **25**, 1895–1899.
41 U. U. Ozkose, C. Altinkok, O. Yilmaz, O. Alpturk and M. A. Tasdelen, *Eur. Polym. J.*, 2017, **88**, 586–593.
42 J.-S. S. Park, Y. Akiyama, F. M. Winnik and K. Kataoka, *Macromolecules*, 2004, **37**, 6786–6792.
43 J. Niu, Z. A. Page, N. D. Dolinski, A. Anastasaki, A. T. Hsueh, H. T. Soh and C. J. Hawker, *ACS Macro Lett.*, 2017, **6**, 1109–1113.
44 V. Najafi, F. Ziaee, K. Kabiri, M. J. Z. Mehr, H. Abdollahi, P. M. Nezhad, S. M. Jalilian and A. Nouri, *Iran. Polym. J.*, 2012, **21**, 683–688.

45 F. Ding, S. Monsaert, R. Drozdzak, I. Dragutan, V. Dragutan, Y. Sun, E. Gao, P. Van Der Voort and F. Verpoort, *Vib. Spectrosc.*, 2009, **51**, 147–151.
46 C. Zhang, R. J. P. Sanchez, C. Fu, R. Clayden-Zabik, H. Peng, K. Kempe and A. K. Whittaker, *Biomacromolecules*, 2019, **20**, 365–374.
47 H.-J. Krause and P. Neumann, Process for the preparation of 2-alkyl- and 2-alkenyl- oxazolines, EP0315856A1, 1988.
48 Y. Seo, A. Schulz, Y. Han, Z. He, H. Bludau, X. Wan, J. Tong, T. K. Bronich, M. Sokolsky, R. Luxenhofer, R. Jordan and A. V. Kabanov, *Polym. Adv. Technol.*, 2015, **26**, 837–850.
49 M. Meyer and H. Schlaad, *Macromolecules*, 2006, **39**, 3967–3970.
50 E. Rossegger, V. Schenk and F. Wiesbrock, *Polymers*, 2013, **5**, 956–1011.
51 O. Celebi, S. R. Barnes, G. S. Narang, D. Kellogg, S. J. Mecham and J. S. Riffle, *Polymer*, 2015, **56**, 147–156.
52 R. Hoogenboom, M. W. M. Fijten, H. M. L. Thijs, B. M. Van Lankvelt and U. S. Schubert, *Des. Monomers Polym.*, 2005, **8**, 659–671.
53 M. Litt, A. Levy and J. Herz, *J. Macromol. Sci., Part A: Chem.*, 1975, **9**, 703–727.
54 D. S. Stephenson and G. Binsch, *J. Magn. Reson.*, 1978, **32**, 145–152.
55 D. Bera, O. Sedlacek, E. Jager, E. Pavlova, M. Vergaelen and R. Hoogenboom, *Polym. Chem.*, 2019, **10**, 5116–5123.
56 J.-S. S. Park and K. Kataoka, *Macromolecules*, 2007, **40**, 3599–3609.
57 P. H. M. M. Van Steenberge, O. Sedlacek, J. C. Hernández-Ortiz, B. Verbraeken, M.-F. Reyniers, R. Hoogenboom and D. R. D'hooge, *Nat. Commun.*, 2019, **10**, 3641.
58 P. H. M. M. Van Steenberge, B. Verbraeken, M.-F. F. Reyniers, R. Hoogenboom, D. R. D'Hooge and D. R. D'hooge, *Macromolecules*, 2015, **48**, 7765–7773.
59 K. Dušek and M. Dušková-Smrčková, *Macromol. React. Eng.*, 2012, **6**, 426–445.